Compositional, Structural and Optical Properties of Cu^{2+} Doped ZnO Nanocrystalline Thin Films

N. Nithya*, S. Rugmini Radhakrishnan**

*Department of Physics, Tamilnadu College of Engineering, Coimbatore, Tamilnadu, 641659, India.
**Department of Physics, Avinashilingam Institute for Home Science and Higher Education for Women, Coimbatore - 641043, Tamilnadu, India.
***Corresponding Author's Email:** nithi2k@yahoo.com

Abstract: Pure ZnO and copper incorporated ZnO thin films with various Cu^{2+} concentrations have been prepared using a new chemical bath deposition route on glass substrate immersed in ammonium solution bath, in which zinc acetate heptahydrate acts as a complexing agent and urea acts as a source of oxide ions. The chemical composition of films was determined by energy dispersive X-ray analyzer (EDAX). The prepared films are very close to ZnO stoichiometry and no impurity compounds such as $Zn(OH)_2$ or CuO species were observed. The pure and Cu doped ZnO structures were characterized by X-ray diffraction (XRD), and transmission electron microscopy (TEM). The XRD results revealed that prepared nanocrystalline films have wrutzite structure and the unit cell volume increased with increasing Cu concentration. Optical properties of the synthesized nanocrystalline were investigated by UV-Vis. spectroscopy and room temperature photoluminescence (PL) spectroscopy. It is seen that the optical band gap increases when the ZnO is doped with copper. Room temperature PL spectra of these structures showed a strong UV emission peak and a relative broad emission peak, and the UV emission peak of the doped ZnO nanocrystalline films was red-shifted with respect to that of the pure ZnO nanocrystalline film.

Keywords: Nanocrystalline film, chemical bath deposition, XRD, UV-Vis., photoluminescence

Accepted On: 26.11.2013

1. Introduction

Zinc oxide (ZnO) is one of the most promising materials for the application of piezoelectric, optoelectronics, chemical sensors and solar cells [1, 2, 3] and for the fabrication of optoelectronic devices operating in the blue and ultra-violet (UV) region, owing to its direct wide band gap (3.37 eV) and large exciton binding energy (60 meV) [4]. Apart from the technological significance of the ZnO nanostructures, their quasi-one-dimensional structure with diameters in the range of tens to hundreds of nanometers makes them interesting from a scientific point of view. ZnO nanocrystalline films may have more novel optical and electrical properties than bulk crystals owing to quantum confinement effects. So far, more unique behaviors are continuously being explored [5,6,7,8]. Further understanding the structural and optical characterizations of ZnO nanoparticles is important for fundamental science and photonic application. For the wide variety of applications and novel properties, various methods have been used to prepare ZnO nanocrystalline films. Sputtering [9], thermal evaporation [10], and chemical vapor deposition (CVD) [11] need expensive equipments, which increase the costs. Compared with these physical methods, chemical bath deposition (CBD) method is widely adopted for the fabrication of ZnO due to its simplicity, safety, no need of costly vacuum system and a cheap method for large area coating [12, 13].

Many researchers [14,15,16] observed that a small amount of doping would create additional carriers in doped ZnO, and its optical properties would be greatly enhanced in bulk samples. A lot of evidences of electrical and magnetic behavior have been reported for ZnO doped with transition metal (TM) like Mn, Co, V, Cu and Fe, indicating significant influence of the TM ions on the ZnO based II – VI semiconductor nanoparticles [17,18,19]. The role of copper as a luminescence activator and a consequence of n-type material is of considerable significance for II–VI semiconductor compounds for its use in industry as information storage materials, coating materials of fluorescent lamps, control panel displays, plasma display panels, field effect transistor, solar cell panel etc. Recently, many researchers have tried to dope different concentration of TM ions into the ZnO based semiconductors to change their optical and magnetic properties by introducing additional carriers [20,21,22]. Cu^{2+}

doped ZnO ($ZnO:Cu^{2+}$) thin films are the most attractive materials, as they can substitute the transparent conducting material (TCO), which can be largely used in optoelectronic devices and solar cell panels. However to our knowledge little work has been devoted to Cu^{2+} doped ZnO nanocrystalline films.

In the present work, we report the influence of different concentration of Cu^{2+} doping on the structural and optical properties of ZnO nanocrystalline films prepared by chemical bath deposition technique.

2. Experimental

2.1. Preparation of Cu2+ doped ZnO Nanocrystalline Films

The different concentration of (2.5, 5.0, 7.5 and 10.0 mole %) Cu^{2+} doped ZnO nanocrystalline films were prepared by using chemical bath deposition method. The raw materials $Zn(CH_3COO)_2.7H_2O$, $CuCl_2$, NH_4OH and $CO(NH_2)_2$ were analytically pure grade purchased from Sigma-Aldrich Company and used without any further purification. The depositions take place on commercial glasses. These were cleaned with detergent in an ultrasonic cleaner and finally dried with N_2. Firstly, proper quantities of $Zn(CH_3COO)_2.7H_2O$ and $CuCl_2$ (2.5, 5.0, 7.5 and 10.0 mole %) were thoroughly mixed with $CO(NH_2)_2$ according to the desired stoichiometry (1:1). Then the mixture was dissolved into 50 ml deionized water to get homogeneous mixture solution. With stirring, few drops of NH_4OH solution were added into the mixture solution in order to maintain the pH at 9. Heating the liquid phase at 60 ºC with continuous stirring for about 70 minutes to produce $ZnO:Cu^{2+}$ nanoparticles. After that the solution was stirred for few seconds and then transferred into another beaker containing cleaned glass substrate placed vertically inside the beaker. The bath was kept at room temperature (30 ºC) for 3 h.

In order to maintain uniform thickness of the $ZnO:Cu^{2+}$ nonocrystalline films for all the concentration of dopant, the coating time is maintained as 3 h. After the deposition, the substrate coated with films was taken out, washed with double distilled water and acetone, and then dried in hot oven at 60 ºC for an hour. The photograph of the synthesized pure and Cu^{2+} doped ZnO nanocrystalline films are shown in Fig. 1.

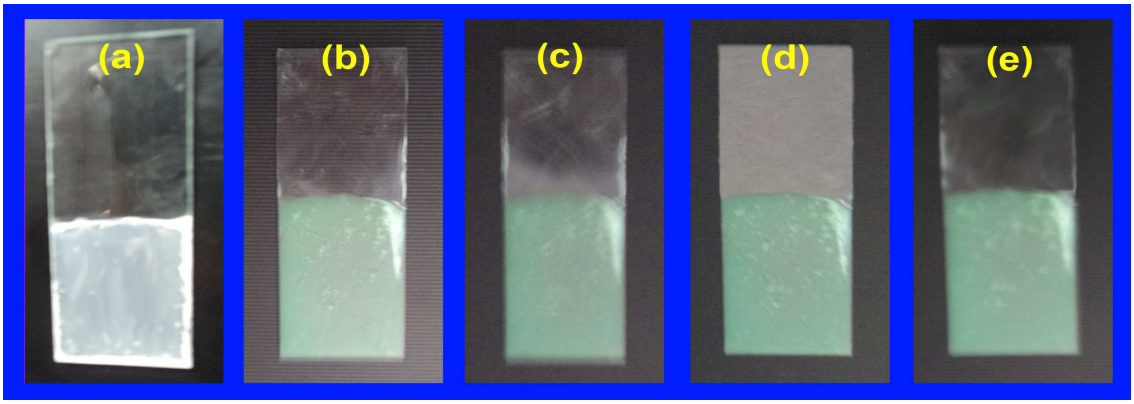

Fig. 1. Photograph of the synthesized (a) pure ZnO (b) 2.5 mole % Cu^{2+} doped ZnO (c) 5.0 mole % Cu^{2+} doped ZnO (d) 7.5 mole % Cu^{2+} doped ZnO (e) 10.0 mole % Cu^{2+} doped ZnO nanocrystalline films

2.2. Reaction Protocol

This method is based on the sequence of reaction on the glass substrate surface. $ZnO:Cu^{2+}$ is formed by the following reaction

$$(CH_3COO)_2Zn \rightarrow 2CH_3COO^- + Zn^{2+}$$

Urea has been used as the O^{2-} source through hydrolysis in alkaline medium:

$$NH_2-CO=NH_2 + H_2O \rightarrow O^{2-} + H_2O\ Zn^{2+} + O^{2-} \rightarrow ZnO$$

$ZnO:Cu^{2+}$ precipitation can take place even at the lowest Zn^{2+}/Cu^{2+} and O^{2-} ion concentration. The deposition process depends upon bath temperature, metal ion concentration, pH of solution, etc. In the present work, the pH of bath solution was maintained as 9.0 with addition of NH_3OH solution. It was found that with increasing pH, the $ZnO:Cu^{2+}$ formation resulted in to $ZnO:Cu^{2+}$ precipitate in the bulk of solution with no or nonuniform film formation on the substrate. Depending upon bath

temperature, the ZnO:Cu^{2+} film formation was started in about 10 min and completed within 180 min. The solution color was changed from whitish to greenish after deposition.

2.3. Characterization of ZnO:Cu^{2+} Nanocrystalline Film

X-ray diffraction patterns of the synthesized samples were recorded in PANalytical X-Pert Pro diffractometer with Cu Ka radiation (λ = 1.54056 Å) source over the diffraction angle 2θ between 20º and 80º. The film composition was determined by energy dispersive X-ray analyzer (EDX). The surface morphology of as-deposited ZnO and Cu^{2+} doped nanocrystalline films was studied using NT-MDP (Russian Made) Solver Pro-47 (in tapping mode), atomic force microscopy (AFM). The absorption measurements were made by SHIMADZU UV-2400 PC spectrometer with a medium scan speed sampling interval 0.5 nm in the wavelength range 200-800 nm. The photoluminescence (PL) spectra were obtained on a FLUOROLOG-FL3-11 Spectroflorometer with wavelength resolution of 0.5 nm at room temperature. Xenon arc lamp of 450 W was used as the excitation light source. All the PL spectra in this study were acquired at an excitation wavelength of 300 nm.

3. Results and Discussion

3.1 Composition Analysis

Chemical composition of pure ZnO and different concentration of Cu^{2+} doped ZnO nanocrystalline films were analyzed by energy-dispersive X-ray analyzer (EDX). The EDX spectra's of the synthesized undoped and doped ZnO films are shown in Fig. 2a and the corresponding composition data (atomic %) are shown in Fig. 2b. It is understood from the data that our synthesis approach provides more reliable products with respect to the chosen composition. EDX analysis indicated the presence of zinc, copper and oxygen for all the synthesized doped films. It reveals that the different concentration of dopant (Cu^{2+}) clearly incorporated with the host matrix. Furthermore, few weak peaks were observed which are related to their presence in the glass substrate.

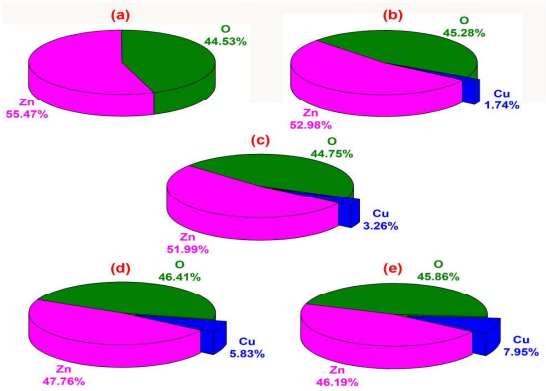

Fig. 2. Material composition (at. %) in the prepared pure and Cu doped nanocrystalline film. (a) pure ZnO (b) 2.5 mole % Cu^{2+} doped ZnO (c) 5.0 mole % Cu^{2+} doped ZnO (d) 7.5 mole % Cu^{2+} doped ZnO and (e) 10.0 mole % Cu^{2+} doped ZnO

3.2. Structural Analysis

Fig. 3 shows the XRD patterns of pure and Cu^{2+} doped ZnO nanostructures. The positions of the diffraction peaks showed that all the films were polycrystalline with a structure that belonged to the ZnO hexagonal wurtzite type (JCPDS no. 36-1451). The broadening of the peaks indicates the prepared film is the nanocrystalline nature. The phases have been clearly indexed, and are shown in Fig. 3. The higher intensity of the (1 0 1) diffraction peak compared with the (1 0 0) and (0 0 2) plane suggested that the nanoparticles exhibited a c-axis preferred orientation. By increasing the copper doping concentration, the reflected intensity at (1 0 1) plane appears to increase. This indicates that most of the have a strong c-axis orientation along (1 0 1) plane normal to the substrate. However, the film deposited with 10 mole % has the higher (1 0 1) intensity. In the recorded XRD spectrum no other peaks are observed, suggesting that only single-phase ZnO has formed. Also, from the recorded spectrums, one can understand that the degree of crystallinity improves with the increasing concentration of dopant in the host ZnO. The observed structural data from the XRD measurements

are summarized in Table 1. From Fig. 3 it reveals that the diffraction peaks gradually shift to lower diffraction with the increase of Cu^{2+} concentration in ZnO lattices. The continuous peak-shift may rule out the phase separation or separated nucleation of CuO and other byproducts of Zn and Cu, the peak broadening and shifting clearly indicates that the addition of dopant may replace the Zn^{2+} site or enter into the interstitial position.

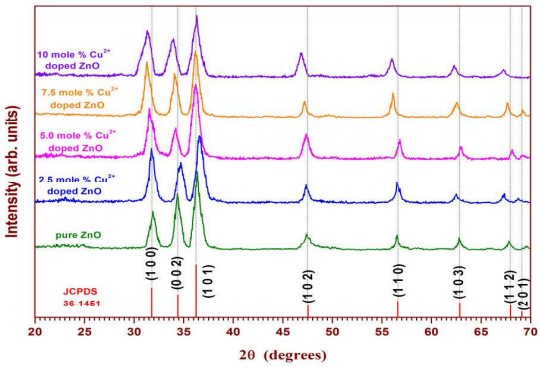

Fig. 3. XRD spectras of pure and different concentration of Cu^{2+} doped ZnO nanocrystalline films

The variation of c/a ratio and unit cell volume expansion features with respect to concentration of Cu^{2+} in ZnO lattices is shown in Fig. 4. The c/a ratio also confirms that the variation is much noticeable particularly for the concentration such as 7.5 and 10.0 mole %. More interestingly, when 'a' is seen enhanced 'c' seems to have dropped, which suggests that the non-uniform lattice expansion in the 'c' axis with respect to 'a' axis of the unit cell. It can also be attributed to the more directional incorporation of the substituting dopant atoms in one axis than the other axis. However when the host atoms (Zn) are substituted by dopant atom (Cu^{2+}) the cell structure with different lattice parameter could occur, such behavior is clearly brought out here. It suggests that Cu^{2+} plays a crucial role in the stacking of substituting atoms in the host lattice, probably through influencing the mobility of substituting atoms.

The variation in the unit cell volume of pure ZnO when adding Cu^{2+} by 2.5, 5.0, 7.5 and 10.0 mole % matrixes has been verified. The variation of unit cell volume with dopant concentrations is shown in Fig. 4. It is clearly observed in Fig. 4 where the unit cell volume is increasing when going from 2.5 mole % to 10.0 mole %, for Cu^{2+} is assigned to replace Zn^{2+} sites. In spite of the decrease in 'a' or'c', the overall cell volume has never been observed to drop. If directional growth occurs during substitution, the lattice parameter decreases in one direction would be compromised by the increased lattice in other direction. Therefore it is logical to presume that the lattice growth is more towards 'c' direction than 'a' direction. This nice trend of almost uniform cell volume expansion (see Fig. 4) reveals Cu^{2+} as a chemical species playing a role in the stacking but does not hinder the occupancy in Zn^{2+} sites.

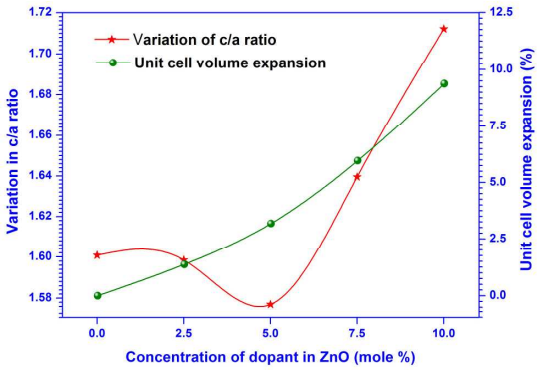

Fig. 4. The variation c/a ratio and unit cell volume expansion with various Cu^{2+}concentrations (mole %) in ZnO.

The crystallite size (D) for pure and Cu^{2+} doped ZnO nanocrystalline films are calculated by using the Debye-Scherrer's formula [23]. The calculated average crystallite sizes of pure and doped ZnO.

Table 1. The observed structural data from XRD measurements for pure and doped ZnO nanocrystalline film. (*obtained from JCPDS file No. 36-1451)

Sample name	Dopant concentration	Calculated parameters		
	Mole %	a=b (Å)	c (Å)	Volume (Å^3)
pure ZnO	–	3.2414 *3.2498	5.1887 *5.2066	47.212 *47.621
ZnO:Cu^{2+}	2.5	3.2576	5.2074	47.857
	5.0	3.2918	5.1911	48.714
	7.5	3.2784	5.3751	50.031
	10.0	3.2657	5.5912	51.640

nanocrystalline films are given in Table 2. The crystallite sizes are found to increase with the increase of dopant concentration in the host ZnO. With the increase of dopant concentration in the host ZnO solutions larger number of Cu^{2+} ions are enter into unit cell and replace the host Zn^{2+} site resulting in the increase of crystallite sizes. It is found that the unit cell volume of the pure ZnO nanocrystalline film deviates from its bulk value (47.62 Å^3).

Table 2. Calculated crystallite sizes for pure and doped ZnO nanocrystalline films (from XRD)

Sample name	Dopant concentration	Crystallite size	Particle size
	Mole %	nm	nm
pure ZnO	–	7.21	10.2
ZnO:Cu^{2+}	2.5	7.83	–
	5.0	9.18	–
	7.5	10.36	–
	10.0	11.29	14.12

As the incorporation of Cu^{2+} in the host ZnO lattices, the diffraction peaks become narrower due to an expansion in the grain size. The highest value of crystallite size calculated for ZnO:Cu^{2+} (10 mole %) was found to be 11.29 nm. It is also noted that the intensity of the diffraction peaks decreases after doping also slightly shifted in lower angle side (see Fig. 3). This can be attributed to doping induced structural disorder in the parent ZnO lattices. This confirms the formation of ZnO:Cu^{2+}; because when Cu^{2+} occupies the Zn^{2+} sites in the lattice , the lattice would undergo a expansion due to higher ionic radii of Cu^{2+} (0.91 Å) than that of the ionic radii of Zn^{2+} (0.83 Å). Therefore the crystallite size of doped ZnO was slightly increased when compared from the host ZnO nanocrystals. The substitution of Cu^{2+} for Zn^{2+} sites in parent material is of significant importance in few areas.

Apart from the crystal structure and crystallite size analysis, yet another important structural characteristic of nanomaterials relates to the gross structural/morphological properties. Smaller sized nanoparticles, with their high surface energy often adhere to the neighboring particles, thus appear like bigger particles [24]. The AFM images were recorded for pure ZnO and 10.0 mole % Cu^{2+} ZnO doped nanocrystalline films. The two dimensional images, three dimensional images and particle size distribution histograms are shown in Fig. 5. From the AFM images it reveals that the prepared nanocrystalline films are uniform, dense and well packed between particles. Particle sizes have been calculated from the particle size distribution histograms. From the particle size histograms (Fig. 5) it reveals that the presence of small sized particles is dominant in all the cases, there is a small variation

in the overall particle sizes. This is the clear indication that uniformity is indeed a big case in all samples regardless of what the dopant concentration is employed in the host ZnO lattices. Clearly, from the comparison of AFM images it is clear that, there is only a small variation of height and depth which is the indication of smooth surface morphology of the nanocrystalline films. The calculated particle sizes are given in Table 2.

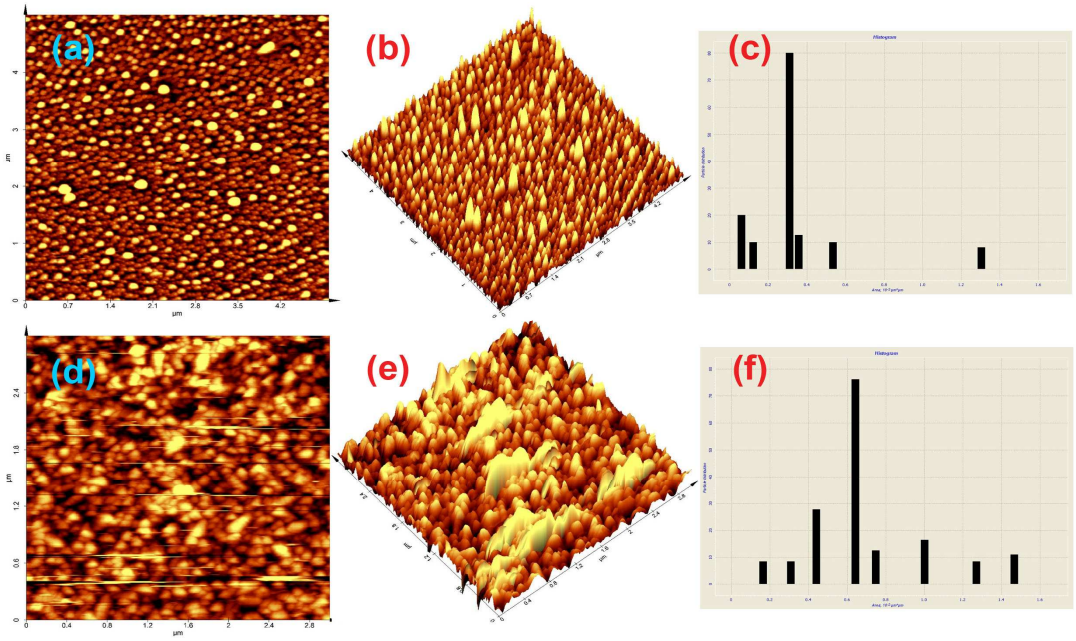

Fig. 5. AFM images of pure and 10 mole % Cu^{2+} doped ZnO nanocrystalline film. [a] 2D image of pure ZnO [b] 3D image of pure ZnO [c] particle size distribution histogram of pure ZnO [d] 2D image of 10 mole % Cu^{2+} doped ZnO [e] 3D image of 10 mole % Cu^{2+} doped ZnO [f] particle size distribution histogram of 10 mole % Cu^{2+} doped ZnO

3.3 Optical Analysis

UV–Vis. absorption spectroscopy is an important and useful technique to study the optical properties of semiconducting nanoparticles. The absorbance is expected to depend on several factors such as band gap, oxygen deficiency, size and structure of nanoparticles, surface roughness and impurity centers [25]. A plot of optical absorbance spectra of undoped and Cu^{2+} doped ZnO nanoparticles as a function of the wavelength is shown in Fig. 6. It shows strong absorption in UV region. The absorption edges are found to shift towards higher wavelengths i.e. lower energies with increase in Cu^{2+} concentration in ZnO. The excitonic absorption peak for pure ZnO nanocrystalline film is observed at 341 nm. This is lower than the band gap wavelength of 388 nm for bulk ZnO [26]. Fig. 7 shows the plots of $(\alpha h\upsilon)^2$ *vs* $h\upsilon$ for pure ZnO, and Cu^{2+} doped ZnO nanocrystalline films. The linear variation of $(\alpha h\upsilon)^2$ *vs* $h\upsilon$ at the absorption edge, confirmed the semiconducting behavior of the film with direct band gap. Extrapolating the straight line portion of the plot $(\alpha h\upsilon)^2$ versus $h\upsilon$ for zero absorption coefficient value gives the optical band gap (E_g). The 'E_g' value of pure ZnO thin film is 3.37 eV and Cu^{2+} doped ZnO film is decreases with the increasing dopant concentration. The obtained energy gap values are in good agreement with ZnO nanoparticles [27]. The shifting of band gap towards lower energy value (red shift) confirms the dopant entered into the host Zn^{2+} lattices. Also it reveals that the addition of dopant increases the particle size of doped crystalline film. The substitution of dopant (Cu^{2+}) in Zn^{2+} sites continuously leads to red shift and results in low band gap energy (3.30 eV). The substitution of Cu^{2+} in Zn^{2+} sites reduces the band gap value of host ZnO. While the concentration of dopant (Cu^{2+}) in the host ZnO crystalline film increases from 2.5 mole % to 10.0 mole % the bandgap energy to vary from 3.64 eV to 2.77 eV. The pure ZnO nanocrystalline film has no remarkable absorption in visible light region with a wavelength above 400 nm, whereas the Cu^{2+} doped ZnO nanocrystalline film extends the absorption spectrum obviously into the visible

region. The result indicates the ability of doped ZnO crystalline films to harvest the visible component of solar radiation.

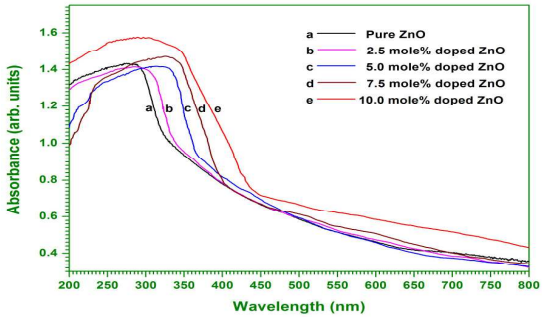

Fig. 6. UV-Vis. absorption spectra of pure and different concentration of Cu^{2+} doped ZnO nanocrystalline films.

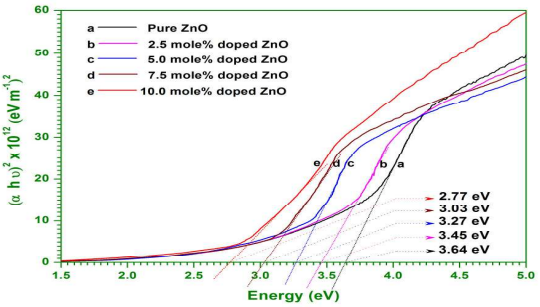

Fig. 7. Plots of $(\alpha h\upsilon)^2$ vs $h\upsilon$ for evaluating the E_g (optical bandgap) values of pure and different concentration of Cu^{2+} doped ZnO nanocrystalline films

As seen in Fig.7, by the addition of Cu^{2+} in host ZnO, the optical band gap energy is greatly reduced when compared to the pure ZnO at all concentration (2.5, 5.0, 7.5 and 10.0 mole %) of dopant. Also it reveals that the decreasing band gap energy of doped nanocrystalline film increases the crystallite sizes. It suggests that Cu^{2+} help to slightly tuning the optical bandgap energy of ZnO. Our optical bandgap energy calculation suggests, for the fabrication of any optical devices which require optical bandgap ranging from a minimum of 2.77 eV to maximum 3.64 eV, the composition and the methods we have described will lend a clue to choose an optimum composition. The E_g value shifted to the longer wavelengths depending upon a number of factors. The shift to the longer wavelength (red shift) generally occurred when the particle size increased [28]. When the particle size was smaller than the Bohr's radius, the blue shift can be explained by the size effect or the effect of quantum confinement [28]. However, the size of all the synthesized films in this experiment is beyond the Bohr's radius, thus the change in E_g values might be influenced by other parameters also. The decrease in E_g for increasing the Cu^{2+} content is attributed to the s–d and p–d interactions giving rise to band gap narrowing and it has been theoretically explained using the second-order perturbation theory [29].

Fig. 8 is the photoluminescence (PL) spectra of pure and Cu^{2+} doped ZnO nanocrystalline films. From the Fig. 8 the PL spectrum of all the as synthesized samples shows the existence of two peaks, a narrow ultra-violet (UV) emission and a broad visible light emission extending from approximately 480 nm to 680 nm with a strong defect emission peak. The narrow ultra-violet emission peak centered at 350 nm (3.54 eV) due to the near band edge emission (NBE) in the wide band gap of ZnO nanoparticle, which resulted from the direct recombination of photo generated charge carriers and is attributed to an exciton- related activity [30, 31]. In the Cu^{2+} doped ZnO nanocrystalline films, the position of near band edge emission peak shift systematically from 364 nm to 392 nm (red shift) with the increase of dopant concentration from 2.5 to 10.0 mole % in steps of 2.5. This significant red shift provides clear evidence for the formation of Cu^{2+} doped ZnO nanocrystalline films. The intensity of ultra violet emission was high for pure and Cu doped ZnO nanocrystalline films, indicating improvement of the crystallinity of pure and doped ZnO nanocrystalline films due to free exciton emission [32]. Moreover, the band edge emission of pure and doped ZnO nanocrystals has a line width (full-width at half maximum) less than 34 nm. This small line width indicates that the as synthesized nanocrystals have a very narrow size distribution.

The strong and broad visible light emission peak (green emission) centered at 541 nm for pure ZnO nanocrystalline film is attributed due to oxygen interstitials and vacancies [33], donor–acceptor transitions [34], zinc vacancies [35] and surface defects [36] in the ZnO lattices. The broad visible light emission band for doped ZnO nanocrystalline film is slightly shifted from 549 nm (green emission, 2.26 eV) for 2.5 mole % Cu^{2+} doped ZnO to 591 nm (orange emission, 2.10 eV) for 10 mole % Cu^{2+} doped ZnO with respect to the varying concentration of dopant (2.5, 5.0, 7.5 and 10.0 mole %) in the host ZnO lattices. As can be noticed in Fig.8 the broad visible light emission peak intensity decreases with increasing dopant concentration in host ZnO films. This can be referred to the fact that the surface per volume ratio of doped ZnO nanocrystals is lesser than that of pure ZnO nanocrystals. This confirms that the binding between Zn ions and surface ligand is different from that of Cu ion. The obtained results not only prove that the dopant entered into the host lattices also show that their optical properties can be effectively tuned for desired emission wavelengths.

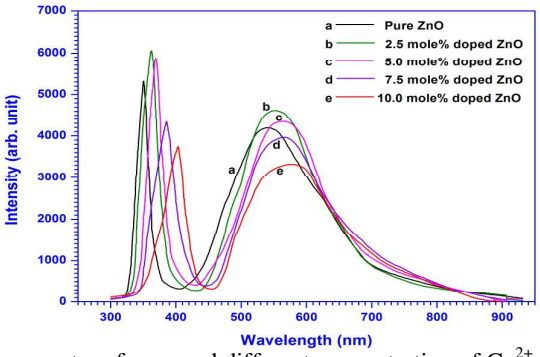

Fig. 8. Photoluminescence spectra of pure and different concentration of Cu^{2+} doped ZnO nanocrystalline films.

Fig. 9 shows the variation of PL intensity of band-edge emission and defect state emission (visible light emission) with different and different concentration of dopant in ZnO nanocrystals. From the figure it reveals that the intensity of all the synthesized nanocrystalline films were high. The strong room-temperature UV emission intensity should be attributed to the high purity and perfect crystallinity of the synthesized nanocrystalline film [37]. The presence of small amount of doapnt greatly affects the PL intensity of ZnO nanocrystalline film. The 2.5 and 5.0 mole % Cu^{2+} doped ZnO nanocrystalline film leads to strong enhancement in photoluminescence yield compared to pure ZnO. The doped ZnO nanocrystalline films are the new useful materials for photonic applications.

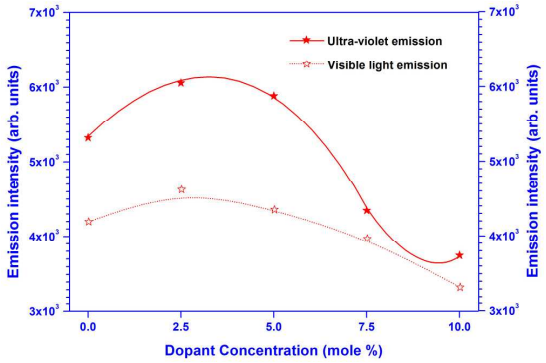

Fig. 9. Variation of PL intensity with concentration of Cu^{2+} in ZnO nanocrystalline film

4. Conclusions

In the present work, we have attempted to prepare and characterize pure and Cu^{2+}doped ZnO nanocrystalline films with different dopant concentrations viz. 2.5, 5.0, 7.5 and 10.0 mole % were prepared by the simple chemical bath deposition method with the easily available chemicals. The stoichiometric concentration of dopant in ZnO nanocrystalline film is also estimated from EDX analysis. The addition of Cu^{2+} slightly decreases the bandgap energy values and is found to be varied

from 3.45 to 2.77 eV with the increasing dopant concentrations. The Cu^{2+} doped ZnO nanocrystalline film extends the absorption spectrum into the visible region and harvest the visible component of solar radiation. The PL spectrum shows the existence of two peaks, a narrow ultra-violet (UV) emission and a broad visible light emission extending from approximately 480 nm to 680 nm with a strong defect emission peak. The position of near band edge emission peak shifts systematically from 364 nm to 392 nm (red shift) with the increasing dopant concentration. The 2.5 and 5.0 mole % Cu^{2+} doped ZnO nanocrystalline film leads to strong enhancement in photoluminescence yield compared to pure ZnO. The doped ZnO nanocrystalline films are the new useful materials for photonic and solar cell applications.

References:

[1] R. Yousefi, A.K. Zak, F. Jamali-Sheini, Ceramics International 39 (2013) 1371–1377.
[2] X. Zi-qiang, D. Hong, L. Yan, C. Hang, Materials Science in Semiconductor Processing 9 (2006) 132–135.
[3] Z. Pan, X. Tian, S. Wu, C. Xiao, Z. Li, J. Deng, G. Hu, Z. Wei, Superlattices and Microstructures 54 (2013) 107–117.
[4] F. Wang, Z. Ye, D. Ma, L. Zhu, F. Zhuge, J. Crystal Growth 283 (2005) 373.
[5] H.M. Cheng, K.F. Lin, H.C. Hsu, W.F. Hsieh, Applied Physics Letters 88 (2006) 261909.
[6] M.K. Patra, M. Manoth, V.K. Singh, G.S. Gowd, V.S. Choudhry, S.R. Vadera, N. Kumar, Journal of Luminescence 129 (2009) 320.
[7] X.Q. Zhang, S.L. Hou, H.B. Mao, J.Q. Wang, Z.Q. Zhu, Applied Surface Science 256 (2010) 3862.
[8] H. Wei, M. Li, Z. Ye, Z. Yang, Y. Zhang, Materials Letters 65 (2011) 427.
[9] W.M. Li and H.Y. Hao, Journal of Materials Science 47 (2012) 3516.
[10] F.Z. Wang, H.P. He, A.A. Ye, L.P. Zhu, J. Appl. Phys. 98 (2005) 084301.
[11] J.P. Biethana, V.P. Sirkeli, L. Considinea, D.D. Nedeoglob, D. Pavlidisa, H.L. Hartnagel, Materials Science and Engineering B 177 (2012) 594.
[12] L.L. Yang, Q.X. Zhao, Magnus Willander, Journal of Alloys and Compounds, 469, 623-629, 2009.
[13] Y. Wang, X. Cui, Y. Zhang, X. Gao, Y. Sun, Journal of Materials Science & Technology, 29, 123-127, 2013.
[14] C.C. Vidyasagar, Y. Arthoba Naik, T.G. Venkatesh, R. Viswanatha , Powder Technology, 214, 337-343, 2011.
[15] M. Khatamian, A.A. Khandar, B. Divband, M. Haghighi, S. Ebrahimiasl, Journal of Molecular Catalysis A: Chemical, 365, 120-127, 2012.
[16] L.F. Koao, F.B. Dejene, H.C. Swart, J.R. Botha (2013) Journal of Luminescence, 143, 463-468
[17] R. Elilarassi, G. Chandrasekaran (2011) Materials Science in Semiconductor Processing, Volume 14, 179-183
[18] E.R. Shaaban, M. El-Hagary, M. Emam-Ismail, A. Matar, I.S. Yahia (2013) Materials Science and Engineering: B, 178, 183-189
[19] R. Saleh, N. F. Djaja, S. P. Prakoso, Journal of Alloys and Compounds, 546, 48-56, 2013.
[20] G.R. Li, D.L. Qu, W.X. Zhao, Y.X. Tong, Electrochemistry Communications 9 (2007) 1661.
[21] N. Brihi, A. Bouaine, A. Berbadj, G. Schmerber, S. Colis, A. Dinia, Thin Solid Films 518 (2010) 4549.
[22] D. Chakraborti, S. Ramachandran, G. Trichy, J. Narayan, Journal of Applied Physics 101 (2007) 053918.
[23] B.E. Waren, X-ray Diffraction, Addison-Wesley, Reading, MA, 1969.
[24] R.Vogel, P. Hoyer and H. Weller , J. Phys. Chem. 98, (1994) 3183-3188
[25] A.S. Ahmed, M.M. Shafeeq, M.L. Singla, S. Tabassum, A.H. Naqvi, A. Azam, J. Lumin. 131 (2010) 1.
[26] P. Kumbhakar, D. Singh, C. S. Tiwary, A. K. Mitra, Chalcogenide Lett. 5 (2008) 387–394.
[27] K.F. Lin, H.M. Cheng, H.C. Hsu, L.J. Lin, W.F. Hsieh, Chemical Physics Letters 409 (2005) 208–211

[28] S. Suwanboon, P. Amornpitoksuk, A. Haidoux, J.C. Tedenac, Journal of Alloys and Compounds 462, 335–339, 2008.
[29] R.B. Bylsma, W.M. Becker, J. Kossut, U. Debska, Phys. Rev. B 33, 8207–8215, 1986.
[30] C.-F. Yu, C.-W. Sung, S.-H. Chen, S.-J. Sun, Appl. Surf. Sci. 256, 792–7969, 2009.
[31] S. Wei, J. Lian, H. Wu, Mater. Charact. 61, 1239–1244, 2010.
[32] Y Zhang, G Du, X Yang, B Zhao, Y Ma, T Yang, H.C Ong, D Liu, S Yang, Semicond. Sci. Technol. 19, 755–758, 2004.
[33] J Yang, J Lang, C.L Yang, Q Han, Y Zhang, D Wang, M Gao, X Liu, Appl. Surf. Sci. 255, 2500–2503, 2008.
[34] D.C Reynolds, D.C Look, B Jogai, J. Appl. Phys. 89, 3 – 9, 2001.
[35] O.D Jayakumar, V Sudarsan, C Sudakar, R Naik, R.K Vatsa, A.K Tyagi, Scr. Mater. 62, 662–665, 2010.
[36] A.B Djurišic´, W.C.H Choy, V.A.L Roy, Y.H Leung, C.Y Kwong, K.W Cheah, T.K Gundu Rao, W.K Chan, H Fei Lui, C Surya, Adv. Funct. Mater. 14, 856–864, 2004.
[37] S Maensiri, C Masingboon, V Promarak, S Seraphin, Optik. Mater. 29, 1700–1705, 2007.